*Clays and Clay Minerals*, Vol. 38, No. 2, 196–202, 1990.

# THE INFLUENCE OF ALUMINUM ON IRON OXIDES: XIV. AL-SUBSTITUTED MAGNETITE SYNTHESIZED AT AMBIENT TEMPERATURES

U. SCHWERTMANN AND E. MURAD

Lehrstuhl für Bodenkunde, Technische Universität München
D-8050 Freising-Weihenstephan, Federal Republic of Germany

**Abstract**—Mixtures of magnetite and goethite were formed by the slow oxidation of mixed $FeCl_2$-$AlCl_3$ solutions in an alkaline environment at room temperature. The compositions of the products ranged from almost exclusively magnetite in Al-free systems to goethite only at Al/(Al + Fe) ≈ 0.3. The magnetic phase consisted of a partly oxidized ($Fe^{2+}/Fe^{3+} < 0.5$), Al-substituted magnetite. The unit-cell edge length $a$ of the magnetite decreased with increasing Al (Al = 0–0.37 per formula unit, corresponding to 0–14 mole % Al) and decreasing $Fe^{2+}$ in the structure as described by the empirical relationship $a(A) = 8.3455 + 0.0693\ Fe^{2+} - 0.0789$ Al. A correlation between the experimentally determined $a$ and that calculated from the unit-cell edge lengths of end-member magnetite, maghemite, and hercynite was highly significant (r = .96) although shifted by about 0.01 Å. Mössbauer spectra showed Al to have entered preferentially the tetrahedral rather than the octahedral sites at low Al substitutions (<0.15 per formula unit), perhaps because of steric reasons. With increasing Al substitution the crystal size of magnetite decreased and structural strain increased, indicating that the structure had a limited capability to incorporate Al under these synthesis conditions. The capacity of the goethite structure to tolerate more Al may explain why goethite replaced magnetite at higher Al concentrations.

**Key Words**—Aluminum, Goethite, Iron oxide, Magnetite, Mössbauer spectroscopy, X-ray powder diffraction.

## INTRODUCTION

Al-substituted goethite and hematite are readily synthesized from aqueous solutions at temperatures <100°C. Al-substituted goethite forms instead of Al-substituted lepidocrocite if Al-containing $FeCl_2$ solutions are oxidized at neutral pH (Taylor and Schwertmann, 1978; Fey and Dixon, 1981), whereas as much as 10 mole % Al can be incorporated in lepidocrocite at pH 8 (Schwertmann and Wolska, 1990). The oxidation of $FeCl_2$ at pH >8 leads to the formation of magnetite. The influence of Al on such a system has not yet been investigated.

To our knowledge, Al-for-Fe substitution in magnetites has so far only been achieved by reducing $(Fe,Al)_2O_3$ with $H_2$ at 400°C (Michel and Pouillard, 1949) or by sintering mixed Al and Fe salts at about 1300°C in a controlled atmosphere (Dehe *et al.*, 1975; Rosenberg *et al.*, 1985). The present investigation was therefore undertaken to answer the following questions: (1) Does Al inhibit magnetite formation under alkaline conditions at ambient temperatures? (2) In magnetite formed under these conditions, is Al incorporated into the structure? (3) If so, what are the effects of incorporated Al on unit-cell edge lengths, particle size, and strain in the magnetite crystals?

## EXPERIMENTAL

### *Sample syntheses*

One-liter batches of mixed 0.05 M $FeCl_2$-$Al(NO_3)_3$ solutions, having Al/(Al + Fe) ratios between 0 and 0.40, were prepared and stored in plastic bottles. The solutions were slowly oxidized at pH 11.7 and room temperature (RT) by daily opening and swirling the contents of the bottles. The total reaction time was between 123 and 155 days. Because the oxidation conditions could not be perfectly controlled, two parallel series of products were prepared having Al/(Al + Fe) ratios in the solution increasing in the range 0–0.40 in relative large steps of 0.05 (series I and II), and three series (III–V) were prepared having Al/(Al + Fe) in the range 0–0.13 with smaller steps of about 0.02–0.04. An additional series (series 0.2) was synthesized for 26 days from 0.01 M $FeCl_2$-$Al(NO_3)_3$ solution (instead of 0.05 M), and another, from 0.05 M solutions, at 80°C for 28 days (series 80). For these last two series, the pH was also readjusted to 11.7 from time to time. The end-products were centrifuged, thoroughly washed, dried at 40°C, and gently powdered.

### *Sample analyses*

The chemical compositions of magnetites in the magnetite-goethite mixtures were derived from the

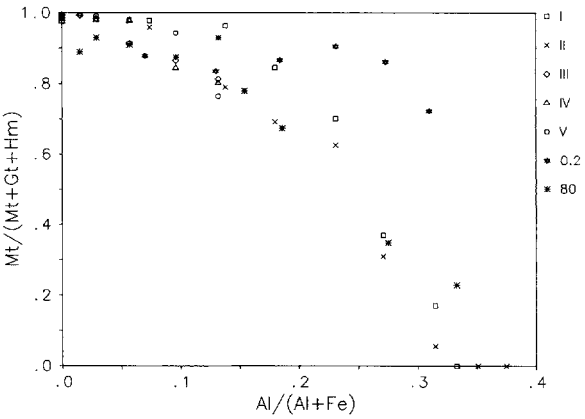


Figure 1. Proportion of magnetite (Mt) in the synthesis products as a function of Al/(Al + Fe) in the system for the various synthesis series. Gt = goethite, Hm = hematite.

analyses of extracts obtained by treating about 20 mg of sample with 50 ml of 1.8 M $H_2SO_4$ at 50°C. Dissolution-time curves and X-ray powder diffraction (XRD) showed that under these conditions magnetite dissolved much more rapidly than goethite. A separation of the two phases was therefore possible after an extraction time of 5 hr. The $H_2SO_4$ extract was analyzed for total Fe by atomic absorption spectrometry, for $Fe^{2+}$ using $\alpha,\alpha'$-dipyridyl, and for Al using aluminon; $Fe^{3+}$ was taken as total Fe minus $Fe^{2+}$. The Fe and Al contents of goethites freed from magnetite as described above were determined after complete dissolution in warm 6 M HCl. Some samples were also analysed for Cl using ion chromatography after dissolution of the magnetite in 0.1 M oxalic acid (20–50 mg sample + 25 ml oxalic acid, 2 hr at RT).

The proportions of magnetite in the magnetite-goethite mixtures were quantified by XRD using the peak intensity (peak height times width at half maximum) of the 220 line of magnetite multiplied by 3.3 and the 110 line of goethite (neglecting a possible influence of Al substitution on peak intensity). The magnetite unit-cell edge lengths $a$ were determined from the positions of the 220, 111, 311, 400, 511, 440, and 422 lines, using 10% Si as an internal standard and a least-squares fitting procedure. In the same way the goethite unit-cell edge lengths $a$, $b$, and $c$ were derived from 6–17 XRD lines, depending on the goethite concentration.

To calculate the effective particle size and strain of the cubic phase, the widths at half maximum of the above-mentioned lines were used, after a quadratic correction for instrumental line broading, by applying the following equation (Klug and Alexander, 1974, p. 665):

$$\frac{(\delta 2\theta)^2}{\tan^2\theta_0} = \frac{K\lambda}{L}\left[\frac{\delta 2\theta}{\tan\theta_0 \sin\theta_0}\right] + 16\,e^2. \qquad (1)$$

This equation is valid provided the particle size-determined line profile is Cauchy and the strain profile is Gaussian. In the equation, $\delta 2\theta$ is the corrected width at half intensity in $^\circ 2\theta$, $\theta_0$ is the position of the line in $^0\theta$, K is a constant taken to be equal to unity, $\lambda$ is the wavelength, L is the mean dimension of the crystallites (MCD), and e (=$\Delta$d/d, where d is the lattice spacing) in the strain. A plot of the left side of Eq. (1) against the term in brackets on the right side yields K$\lambda$/L as the slope and 16 $e^2$ as the intercept of a linear relation from which L and e can be calculated.

For Mössbauer spectroscopy, a $^{57}$Co/Rh source with an activity of about 20 mCi was moved in a sinusoidal mode. Measurements were carried out at room temperature on absorbers containing 20 mg sample placed in a Plexiglas holder having an area of 2 $cm^2$, which gave average Fe concentrations of about 7 $mg/cm^2$. The transmitted radiation was recorded with a Kr-filled proportional counter and stored in a 1024 channel analyzer. Spectra were taken in the velocity range ± 10.5 mm/s until sufficiently good statistics, monitored with an oscilloscope, had been attained. A 6-$\mu$m-thick metallic iron foil served for velocity calibration and as isomer shift reference. Mirror halves of the spectra were folded and Lorentzian line fits carried out by a computer procedure, with corresponding lines within every component sextet constrained to have equal widths and intensities.

## RESULTS AND DISCUSSION

### *Mineralogical composition*

At room temperature goethite and magnetite were the only phases in the end-product, whereas at 80°C, hematite was also formed. In all series the proportion of magnetite decreased and that of goethite (plus hematite in the 80°C series) increased with increasing Al/(Al + Fe) mole ratio (hereafter called Al/(Al + Fe) for brevity) in the total system (Figure 1), although the ratios of the two phases varied somewhat at the same Al/(Al + Fe). The effectiveness of Al in suppressing magnetite thus increased with increasing Al/(Al + Fe). At 0.01 M instead of 0.05 M (Al + Fe), relatively more magnetite was formed at higher Al/(Al + Fe).

### *Compositions and unit-cell edge lengths of magnetite products*

The compositions of the magnetite products, as calculated from chemical analyses, were expressed per 4 oxygens according to the bulk formula $Fe^{2+}_x Fe^{3+}_y Al_z O_4$. Table 1 shows all samples to contain less $Fe^{2+}$ than pure magnetite (x = 1). This deficiency of $Fe^{2+}$ may be due either to partial oxidation of Fe, leading to transitional phases between magnetite and maghemite, and/or to Al-for-$Fe^{2+}$ substitution. The former explanation is favored in view of the fact that x < 1 even if no Al

https://doi.org/10.1346/CCMN.1990.0380211 Published online by Cambridge University Press

had been added. The Al content of the cubic phase increased with added initial Al, whereas $Fe^{2+}$ first increased at low Al concentrations and then decreased.

The unit-cell edge length $a$ should be a function of both the degree of oxidation and Al incorporation, i.e., of x and z in the above formula. For $a$ as a function of the experimentally determined x and z (n = 34), the following multiple correlation was derived:

$$a_{exp}(\text{Å}) = 8.3455 + 0.0693\,x - 0.0789\,z, \quad (2)$$

which explains 93% of the variation of $a$ by the variation of x and z. The intercept of 8.3455 Å derived from Eq. (2) is very close to the unit-cell edge length of maghemite, for which x = z = 0, and agrees exactly with the value recently measured for a natural maghemite from Conakry, Ghana (Schwertmann and Fechter, 1984). Eq. (2) furthermore reflects the increase in $a$ as x ($Fe^{2+}$) increases and the decrease in $a$ as z (Al) increases.

The magnitude of the experimental x and z factors may be compared with theoretical values obtained from the unit-cell edge lengths of the appropriate end member minerals, i.e., magnetite (8.3967 Å; JCPDS 19-62a), maghemite (8.3455 Å; Schwertmann and Fechter, 1984), and hercynite, $Fe^{2+}Al_2O_4$ (8.1558 Å; Hill, 1984). Such a comparison assumes a linear variation of $a$ between the end-members (Vegard rule), which seems justified in view of the dominantly ionic nature of the magnetite structure. The derived theoretical equation is

$$a_{calc}(\text{Å}) = 8.3455 + 0.0512\,x - 0.0949\,z. \quad (3)$$

The correlation between $a_{calc}$ and $a_{exp}$ was highly significant ($a_{exp} = -0.19 + 1.025\,a_{calc}$; n = 33; r = .960); however, Eq. (3) underestimates $a$ significantly by about 0.01 Å, as is apparent if Eqs. (2) and (3) are compared. Thus, the Vegard rule was not strictly obeyed, as has been observed for other Al-substituted Fe(III) oxides synthesized at low temperatures.

One reason for this deviation may be that magnetite is an inverse spinel (in which the divalent cations occupy the octahedral site), whereas hercynite is a normal spinel (in which the divalent cations occupy the tetrahedral site). Another reason could be that OH and/or Cl replaced O in the structure. Featureless IR spectograms in the OH-stretching and -bending range essentially ruled out structural OH. Also, no Cl was detected.

Because of the variation of $a$ with x *and* z, a nonlinear relationship was expected between $a$ and z. The sigmoidal shape of the distribution curves (Figure 2), in fact, shows that $a$ may have even increased slightly with increasing Al substitution at $Al/O_4$ (Al per formula unit) $\lesssim 0.15$. This effect was mainly due to an increase in $Fe^{2+}$ within this range, indicating that the incorporation of Al stabilized $Fe^{2+}$ in the structure. The shape of the curve may, however, also depend on whether Al preferentially occupied tetrahedral or octahedral sites (as in hercynite).

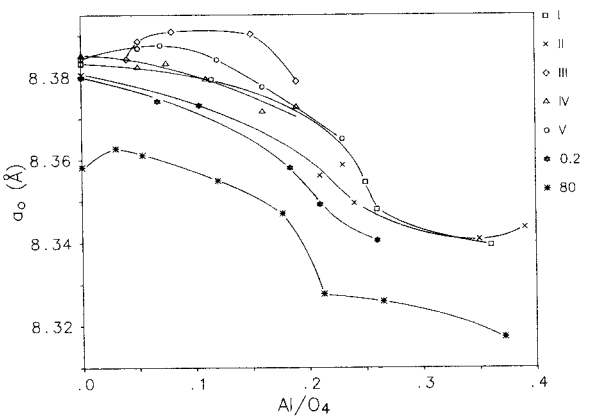


Figure 2. Variation of the magnetite unit-cell edge length $a$ with the $Al/O_4$ (Al per formula unit) ratio z.

The mean crystallite dimension was fairly constant at low substitution, but decreased sharply at a substitution >0.15 $Al/O_4$ (see below). As reported by Schwertmann and Fechter (1984), Al-substituted magnetite phases oxidize to Al-substituted maghemite phases that also have reduced unit-cell size on heating to 250°C.

### *Mössbauer spectra*

Because of electron delocalization on the octahedral sites, the room-temperature Mössbauer spectrum of magnetite comprises two magnetic sextets, one each for $Fe^{3+}$ on the tetrahedral sites and Fe with a nominal average valence of 2.5 on the octahedral sites (Bauminger *et al.*, 1961). For pure, stoichiometric magnetite, the intensity ratio of the tetrahedral to octahedral site resonance is 1:2; the hyperfine fields for these are 49.0 and 46.0 T, and the isomer shifts (relative to metallic Fe) are 0.25 and 0.67 mm/s, respectively. On oxidation of $Fe^{2+}$, electron delocalization on the octahedral sites of magnetites becomes increasingly inhibited, and the $Fe^{2.5+}$ component is gradually replaced by an (additional) sextet due to (excess) $Fe^{3+}$ on the octahedral sites. Annersten and Hafner (1973) showed this octahedral $Fe^{3+}$ sextet to have a hyperfine field that is higher by only 0.3 T than that of tetrahedral $Fe^{3+}$, and the isomer shift to be higher by about 0.14 mm/s. Because of their similar parameters, resolution of the octahedral and tetrahedral $Fe^{3+}$ resonances requires the application of an external magnetic field, which was not available during our study.

Mössbauer spectra of the magnetite products studied here showed the unsubstituted samples of series I, II, IV, and V to have an average total $Fe^{3+}/(Fe^{3+} + Fe^{2.5+})$ ratio of 0.58 ± 0.01 (instead of ideally 0.33). This ratio indicates significant oxidation, i.e., non-stoichiometry. An estimation of the degree of oxidation made on the

https://doi.org/10.1346/CCMN.1990.0380211 Published online by Cambridge University Press

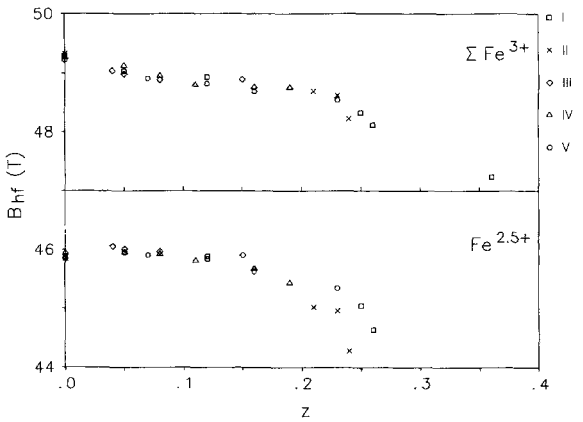


Figure 3. Variation of magnetic hyperfine fields ($B_{hf}$ in Teslas) of total $Fe^{3+}$ and octahedral $Fe^{2.5+}$ of the magnetites with Al substitution.

basis of the relative intensities of the two spectral components (Coey *et al.*, 1971) shows that the Al-free magnetite samples had an average composition of $Fe^{3+}(Fe^{3+}_{1.26}Fe^{2+}_{0.61}\square_{0.13})O_4$, i.e., 39% of the $Fe^{2+}$ had been oxidized. The $Fe^{3+}/(Fe^{3+} + Fe^{2+})$ ratio of 0.78 compares well with that of 0.81 determined chemically. The average hyperfine fields ($B_{hf}$) of the above-mentioned unsubstituted samples were 49.28 ± .04 and 45.88 ± .05 T, and the two sextets had isomer shifts of 0.293 ± .002 and 0.653 ± .011 mm/s, respectively. In agreement with the high $Fe^{3+}$ content of these magnetite phases, the isomer shift of the $Fe^{3+}$ resonance was shifted to a higher value than that of tetrahedral $Fe^{3+}$ (0.25 mm/s; Annersten and Hafner, 1973) and the hyperfine field of the $Fe^{3+}$ resonance was slightly higher than that of stoichiometric magnetite (49.0 T).

The patterns of variation of the magnetic hyperfine field with Al substitution were rather complex. At low Al substitutions ($z < 0.20$), the average $Fe^{3+}$ hyperfine field decreased approximately linearly as a function of z, according to the equation

$$B_{hf} = 49.20 - 2.7\,z, \qquad r = .92,\ n = 17, \qquad (4)$$

with a slope about seven times steeper than that of the $Fe^{2.5+}$ hyperfine field vs. z trend between $0 \le z \le 0.15$ (Figure 3; Table 1). Preferential incorporation of Al in the tetrahedral sites should have led to a more pronounced reduction of the hyperfine field of tetrahedral $Fe^{3+}$ than of the fields ensuing from octahedral $Fe^{3+}$ and mixed-valence $Fe^{2.5+}$. This means that the average octahedral *and* tetrahedral $Fe^{3+}$ hyperfine field (which was observed here) should also have been reduced more than the octahedral $Fe^{2.5+}$ hyperfine field. The more pronounced decrease of the $Fe^{3+}$ resonance thus indicates a preferred substitution of Al in the tetrahedral sites in this substitutional range. At higher Al substitutions, both the total $Fe^{3+}$ and the $Fe^{2.5+}$ hyperfine fields showed a non-linear trend with Al substitution,

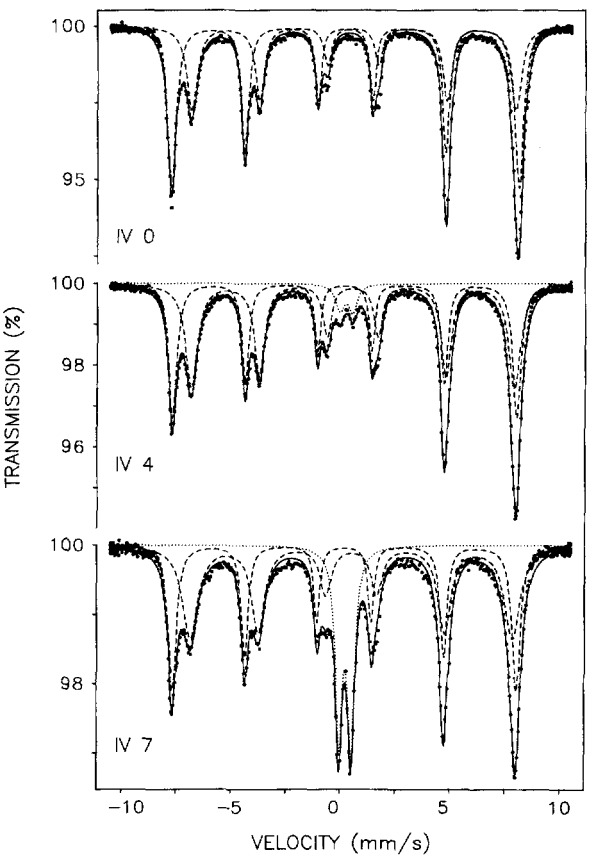


Figure 4. Room-temperature Mössbauer spectra of magnetites from series IV having different Al substitutions (0, 5.7 and 9.6 mole %, respectively, from top to bottom). Magnetic subspectra are plotted with broken lines, paramagnetic subspectra with dotted lines.

decreasing much more strongly than for $z \le 0.15$. For $z > 0.15$, the field of the mixed-valence component furthermore showed a more pronounced dependence on z than the $Fe^{3+}$ field, indicating Al substituting preferentially in the octahedral sites.

The line widths first decreased at low Al substitutions, with minima for the $Fe^{3+}$ resonance at about $z = 0.12$ and for the $Fe^{2.5+}$ sextet at $z = 0.06$. At z values greater than about 0.15, the $Fe^{2.5+}$ resonance began to broaden rapidly and became less well-defined.

The substitution of Fe by Al led to an increasing contribution from the mixed-valence octahedral component, reflecting the increasing $Fe^{2+}$ content shown by chemical analysis and the increase in *a*. Because of the low initial $Fe^{2+}$ content of the magnetites, additional possibilities existed for electron delocalization on the octahedral sites, so that the relative area of the low-hyperfine field component increased (Figure 4). An inhibition of electron delocalization between $Fe^{2+}$ and $Fe^{3+}$ due to an increasing substitution of octahedral $Fe^{3+}$ by Al, which should have weakened the mixed

https://doi.org/10.1346/CCMN.1990.0380211 Published online by Cambridge University Press

Table 1. Proportion, composition, and physical properties of the magnetites.

| Initial Al/(Al + Fe) | Proportion of magnetite (%) | Properties of magnetite $Fe^{2+}_x Fe^{3+}_y Al_z O_4$ | | | | | | | | | |
|---|---|---|---|---|---|---|---|---|---|---|---|
| | | a (Å) | x | y | z | MCD (nm) | Strain $10^4$ | $B(Fe^{3+})^2$ (Tesla) | $I(Fe^{3+})^3$ | $B(Fe^{2.5+})^2$ (Tesla) | $I(Fe^{2.5+})^3$ |
| Series I | | | | | | 0.05 M, RT, 123 days[1] | | | | | |
| 0 | 99 | 8.3833 (3) | 0.50 | 2.33 | 0 | 62.2 | 3.76 | 49.29 (1) | 0.57 | 45.86 (4) | 0.43 |
| 0.074 | 98 | 8.3794 (9) | 0.50 | 2.22 | 0.12 | 49.4 | 3.53 | 48.94 (2) | 0.44 | 45.90 (4) | 0.56 |
| 0.138 | 96 | 8.3546 (3) | 0.48 | 2.10 | 0.25 | 45.3 | 6.17 | 48.33 (3) | 0.41 | 45.05 (7) | 0.59 |
| 0.180 | 85 | 8.3481 (15) | 0.46 | 2.10 | 0.26 | 39.8 | 7.40 | 48.12 (4) | 0.26 | 44.64 (11) | 0.74 |
| 0.231 | 70 | 8.3395 (9) | 0.29 | 2.12 | 0.36 | — | — | 47.24 (9) | 0.23 | 42.8 (3) | 0.77 |
| Series II | | | | | | 0.05 M, RT, 155 days | | | | | |
| 0 | 100 | 8.3806 (1) | 0.48 | 2.35 | 0 | 44.6 | 2.58 | 49.33 (1) | 0.58 | 45.85 (4) | 0.42 |
| 0.074 | 96 | 8.3562 (2) | 0.43 | 2.17 | 0.21 | 47.0 | 7.44 | 48.69 (1) | | 45.02 (7) | |
| 0.138 | 79 | 8.3588 (4) | 0.44 | 2.14 | 0.23 | 42.1 | 8.21 | 48.63 (3) | | 44.96 (12) | |
| 0.180 | 69 | 8.3496 (7) | 0.46 | 2.13 | 0.24 | 37.4 | 10.6 | | | | |
| 0.231 | 63 | 8.3409 (16) | 0.27 | 2.14 | 0.35 | 24.9 | — | | | | |
| Series III | | | | | | 0.05 M, RT, 145 days | | | | | |
| 0.015 | 99 | 8.3844 (2) | 0.64 | 2.20 | 0.04 | 48.5 | 1.15 | 49.04 (2) | 0.46 | 46.06 (3) | 0.54 |
| 0.029 | 98 | 8.3887 (4) | 0.70 | 2.15 | 0.05 | 49.7 | 1.80 | 48.99 (2) | 0.44 | 46.01 (3) | 0.56 |
| 0.057 | 91 | 8.3910 (5) | 0.77 | 2.07 | 0.08 | 72.8 | 4.16 | 48.89 (2) | 0.38 | 45.97 (3) | 0.62 |
| 0.096 | 87 | 8.3904 (6) | 0.70 | 2.05 | 0.15 | 61.3 | 4.82 | 48.90 (4) | 0.32 | 45.91 (6) | 0.68 |
| 0.132 | 81 | 8.3790 (12) | 0.62 | 2.07 | 0.19 | 54.9 | 6.82 | | | | |
| Series IV | | | | | | 0.05 M, RT, 145 days | | | | | |
| 0 | 98 | 8.3852 (3) | 0.56 | 2.29 | 0 | 67.8 | 3.56 | 49.27 (1) | 0.59 | 45.95 (1) | 0.41 |
| 0.015 | 100 | 8.3824 (3) | 0.61 | 2.21 | 0.05 | 50.3 | 2.27 | 49.13 (1) | 0.54 | 45.96 (1) | 0.46 |
| 0.029 | 98 | 8.3833 (2) | 0.65 | 2.16 | 0.08 | 47.5 | 2.29 | 48.96 (1) | 0.48 | 45.93 (2) | 0.52 |
| 0.057 | 98 | 8.3795 (5) | 0.67 | 2.11 | 0.11 | 44.1 | 3.68 | 48.81 (1) | 0.45 | 45.82 (2) | 0.55 |
| 0.096 | 85 | 8.3717 (3) | 0.55 | 2.14 | 0.16 | 59.9 | 6.93 | 48.77 (1) | 0.44 | 45.68 (3) | 0.56 |
| 0.132 | 80 | 8.3728 (15) | 0.54 | 2.12 | 0.19 | 46.5 | 7.14 | 48.76 (2) | 0.29 | 45.44 (4) | 0.71 |
| Series V | | | | | | 0.05 M, RT, 145 days | | | | | |
| 0 | 99 | 8.3846 (6) | 0.57 | 2.28 | 0 | 50.5 | 2.19 | 49.23 (1) | 0.58 | 45.87 (3) | 0.42 |
| 0.015 | 99 | 8.3870 (7) | 0.62 | 2.20 | 0.05 | 58.3 | 3.02 | 49.04 (1) | 0.53 | 45.95 (2) | 0.47 |
| 0.029 | 99 | 8.3877 (7) | 0.70 | 2.12 | 0.07 | 46.7 | 2.47 | 48.91 (1) | 0.47 | 45.91 (2) | 0.53 |
| 0.057 | 98 | 8.3842 (4) | 0.68 | 2.09 | 0.12 | 48.3 | 4.05 | 48.83 (1) | 0.41 | 45.84 (2) | 0.59 |
| 0.096 | 94 | 8.3776 (3) | 0.64 | 2.08 | 0.16 | 41.8 | 5.03 | 48.69 (2) | 0.38 | 45.63 (3) | 0.62 |
| 0.132 | 77 | 8.3651 (7) | 0.59 | 2.04 | 0.23 | 36.2 | 6.22 | 48.55 (2) | 0.36 | 45.35 (6) | 0.64 |
| Series 0.2 | | | | | | 0.01 M, RT, 26 days | | | | | |
| 0 | 100 | 8.3799 (3) | 0.52 | 2.32 | 0 | 49.8 | 2.11 | 49.64 (1) | 0.66 | 45.66 (5) | 0.34 |
| 0.070 | 88 | 8.3742 (4) | 0.47 | 2.29 | 0.07 | 46.2 | 5.46 | 49.17 (3) | | 45.1 (2) | |
| 0.130 | 84 | 8.3732 (3) | 0.51 | 2.23 | 0.10 | 35.3 | 4.92 | | | | |
| 0.184 | 87 | 8.3581 (4) | 0.44 | 2.19 | 0.18 | 25.3 | 5.54 | | | | |
| 0.231 | 91 | 8.3493 (4) | 0.36 | 2.21 | 0.22 | 23.9 | 6.21 | | | | |
| 0.723 | 86 | 8.3406 (3) | 0.31 | 2.20 | 0.26 | 20.1 | 4.73 | | | | |
| 0.310 | 72 | 8.3369 (22) | 0.26 | 2.20 | 0.29 | 21.3 | 6.83 | | | | |
| Series 80 | | | | | | 0.05 M, 80°C, 28 days | | | | | |
| 0 | 98 | 8.3583 (4) | 0.26 | 2.49 | 0 | 73.5 | 5.40 | 49.67 (1) | | 45.80 (6) | |
| 0.015 | 89 | 8.3628 (4) | 0.18 | 2.51 | 0.03 | 72.7 | 4.91 | | | | |
| 0.029 | 93 | 8.3612 (5) | 0.19 | 2.48 | 0.05 | 72.0 | 5.25 | | | | |
| 0.057 | 91 | 8.3550 (4) | 0.19 | 2.42 | 0.12 | 75.9 | 6.41 | | | | |
| 0.096 | 85 | 8.3471 (8) | 0.24 | 2.33 | 0.18 | — | — | | | | |
| 0.132 | 94 | 8.3278 (3) | 0.16 | 2.35 | 0.21 | 38.5 | 5.75 | | | | |
| 0.154 | 78 | 8.3260 (5) | 0.08 | 2.35 | 0.27 | 24.3 | 5.72 | | | | |
| 0.186 | 80 | 8.3174 (3) | 0.10 | 2.23 | 0.37 | 32.3 | 6.82 | | | | |

[1] Series denomination, initial concentration of synthesis solution, synthesis temperature and duration.
B ($Fe^{3+}$), B($Fe^{2.5+}$) = Magnetic hyperfine fields of total $Fe^{3+}$ and mixed valence $Fe^{2.5+}$; errors on last digit given in parentheses.
I($Fe^{3+}$), I($Fe^{2.5+}$) = Relative intensities of the total $Fe^{3+}$ and the mixed valence $Fe^{2.5+}$ resonance; average error ≈ 0.01–0.03.

https://doi.org/10.1346/CCMN.1990.0380211 Published online by Cambridge University Press

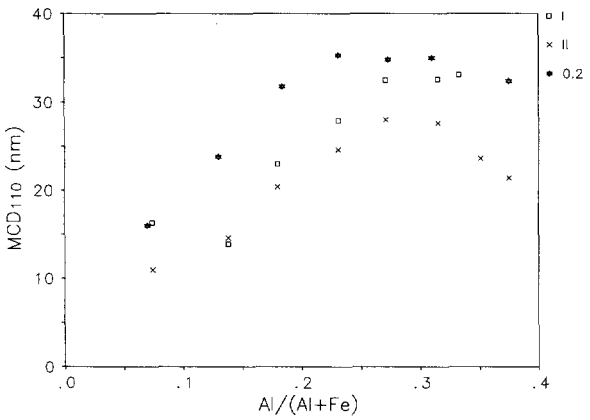


Figure 5. Variation of mean crystallite dimension of goethite perpendicular to 110 ($MCD_{110}$) with the Al/(Al + Fe) ratio in the system.

valence component, was not observed, probably due to the low extent of Al substitution studied here, although the large excess of $Fe^{3+}$ may also have played a role.

Mössbauer spectra of the samples prepared at higher Al concentrations in the synthesis solutions showed an additional (paramagnetic) component. This component had an average quadrupole splitting of 0.59 mm/s and an isomer shift of 0.35 mm/s, and can be essentially assigned to aluminous goethite. No separate tetrahedral $Fe^{2+}$ component, as was described by Dehe *et al.* (1975), was observed in the substitutional range covered.

*Particle size and strain*

The Al-free magnetite crystals varied greatly in size and shape. Small euhedral crystals <100 nm in size were formed together with almost spherical crystals as much as 300 nm in diameter. More uniform but smaller, euhedral crystals (30–60 nm) were formed at Al/(Al + Fe) = 0.14, whereas at Al/(Al + Fe) = 0.23 the crystals had less sharp boundaries and less well-defined shapes. Elongated goethite crystals were also present (see below). Somewhat larger magnetite crystals were obtained at 80°C.

To calculate average strain and mean crystallite dimension (MCD), all XRD lines of the cubic phase were taken as equivalent. A relationship according to Eq. (1) for a particular sample was only considered valid for r > .99. The values for MCD (L) and strain (e) obtained in this way are given in Table 1. In general agreement with electron microscopic observations, the MCDs were negatively correlated with Al substitution, whereas strain showed a positive correlation. The overall correlation was significant, but the coefficients were not very high (r = .68 and −.73, respectively). Introduction of structural $Fe^{2+}$ as a variable did not improve the correlation. The poor correlation could partly have been due to a slight increase in MCD and decrease in strain in the lower substitutional range of some series, possibly connected with the parallel increase in $Fe^{2+}$. A similar phenomenon has been observed for Al-substituted hematite samples (Schwertmann *et al.*, 1979; Murad and Schwertmann, 1986) and goethite samples (Golden, 1978; Schulze and Schwertmann, 1987).

The development of smaller crystals and higher strain at $Al/O_4$ substitutions $\gtrsim$0.10–0.15 may have been caused by the substitution of Al for Fe in octahedral rather than tetrahedral positions. Crystal growth may thus have been impeded by strain, because the difference in bond length between $Fe^{3+}$(VI)–O and Al(VI)–O is about double that between $Fe^{3+}$(IV)–O and Al(IV)–O.

*Goethite*

Chemically determined Al substitutions of the goethite products ranged from 8 to 33 mole %. The generally accepted upper substitutional limit of ⅓ of the Fe atoms thus was not exceeded, even though in some preparations the Al/(Al + Fe) of the starting solutions exceeded 0.33. At these high Al concentrations gibbsite formed instead. The chemically determined Al substitution, $Al_{chem}$, was significantly correlated with that calculated from the unit-cell edge lengths *c*, $Al_c$, (using the equation $Al_c = 1730 - 527\,c$; Schulze, 1984) as follows:

$$Al_c = 2.4 + 0.941\ Al_{chem}, \quad (r = .946, n = 22). \quad (5)$$

At any given Al/(Al + Fe), goethite incorporated more Al in its structure than did magnetite, indicating a higher affinity of Al to the goethite than to the magnetite structure.

MCDs calculated from corrected widths at half height depended strongly on Al/(Al + Fe); see Figure 5. $MCD_{110}$, for example, showed a maximum of about 30 nm at Al/(Al + Fe) ≈ 0.30, where Al substitutions were between 20 and 30 mole %. A similar maximum was recently observed for goethites synthesized from ferrihydrite at 25°C in 0.3 M KOH (Schulze and Schwertmann, 1987). The relatively good crystallinity of the goethites described here is also reflected in Mössbauer spectra of these samples taken between room temperature and 4.2 K (Murad and Bowen, 1987). Thus, Al/(Al + Fe) ratios of 0.2–0.3 appear to be the most favorable for the growth of goethite crystals under the conditions described here; at lower Al/(Al + Fe) ratios magnetite is favored, whereas at higher ratios gibbsite competes with goethite for Al.

Electron micrographs (Schwertmann, 1988) showed two types of crystal shape: spindle-shaped particles 0.2–0.3 μm in length, which were twinned to form more or less complete stars, and thin, rectangular crystals about 0.1 by 0.15 μm in size. All crystals showed striations in the crystallographic *c* direction. Goethite crys-

tals very similar to these in morphology and Al substitution were found in saprolites formed from basalt in southern Brazil (Schwertmann, 1988).

## ACKNOWLEDGMENTS

We are indebted to H. Fechter, B. Gallitscher, and C. Gutbrod for extensive laboratory work, to H. Stanjek for advice on analysis of the XRD data, to H. C. Bartscherer for taking electron micrographs, and to J. M. Bigham for a helpful review of the manuscript. This study was supported by the Deutsche Forschungsgemeinschaft.

## REFERENCES

Annersten, H. and Hafner, S. S. (1973) Vacancy distribution in synthetic spinels of the series $Fe_3O_4$-$\gamma$-$Fe_2O_3$: *Z. Kristallogr.* **137,** 321–340.

Bauminger, R., Cohen, S. G., Marinov, A., Ofer, S., and Segal, E. (1961) Study of the low-temperature transition in magnetite and the internal fields acting on iron nuclei in some spinel ferrites, using Mössbauer absorption: *Phys. Rev.* **122,** 1447–1450.

Coey, J. M. D., Morrish, A. H., and Sawatzky, G. A. (1971) A Mössbauer study of conduction in magnetite: *J. Physique* **32 C1,** 271–273.

Dehe, G., Seidel, B., Melzer, K., and Michalk, C. (1975) Determination of a cation distribution model of the spinel system $Fe_{3-x}Al_xO_4$: *Phys. Stat. Sol.* **31,** 439–447.

Fey, M. V. and Dixon, J. B. (1981) Synthesis and properties of poorly crystalline hydrated aluminous goethites: *Clays & Clay Minerals* **29,** 91–100.

Golden, D. C. (1978) *Physical and chemical properties of aluminum-substituted goethite:* Ph.D. thesis, Department of Soil Science, North Carolina State University, Raleigh, North Carolina, 174 pp.

Hill, R. J. (1984) X-ray powder diffraction profile refinement of synthetic hercynite: *Amer. Mineral.* **69,** 937–942.

Klug, H. P. and Alexander, L. E. (1974) *X-ray Diffraction Procedures for Polycrystalline and Amorphous Materials:* 2nd ed., Wiley, New York, 966 pp.

Michel, A. and Pouillard, E. (1949) Sur une nouvelle famille de sesquioxydes de fer cubiques: *Acad. Sci. Paris, Compt. Rend.* **228,** 680–681.

Murad, E. and Bowen, L. H. (1987) Magnetic ordering in Al-rich goethites: Influence of crystallinity. *Amer. Mineral.* **72,** 194–200.

Murad, E., and Schwertmann, U. (1986) Influence of Al substitution and crystal size on the room-temperature Mössbauer spectrum of hematite: *Clays & Clay Minerals* **34,** 1–6.

Rosenberg, M., Deppe, P., Janssen, H. U., Brabers, V. A. M., Li, F. S., and Dey, S. (1985) A Mössbauer study of Al and Ga substituted magnetite: *J. Appl. Phys.* **57,** 3740–3742.

Schulze, D. G. (1984) The influence of aluminum on iron oxides. VIII. Unit-cell dimensions of Al-substituted goethites and estimation of Al from them: *Clays & Clay Minerals* **32,** 36–44.

Schulze, D. G. and Schwertmann, U. (1987) The influence of aluminum on iron oxides. XIII. Properties of goethites synthesized in 0.3 M KOH at 25°C: *Clay Miner.* **22,** 83–92.

Schwertmann, U. (1988) Some properties of soil and synthetic iron oxides: in *Iron in Soils and Clay Minerals,* J. W. Stucki, B. A. Goodman, and U. Schwertmann, eds., D. Reidel, Dordrecht/Boston, 203–250.

Schwertmann, U. and Fechter, H. (1984) The influence of aluminum on iron oxides. XI. Aluminum-substituted maghemite in soil and its formation: *Soil Sci. Soc. Amer. J.* **48,** 1462–1463.

Schwertmannn, U., Fitzpatrick, R. W., Taylor, R. M., and Lewis, D. G. (1979) The influence of aluminum on iron oxides. II. Preparation and properties of Al-substituted hematites: *Clays & Clay Minerals* **27,** 105–112.

Schwertmann, U. and Wolska, E. (1990) The influence of aluminum on iron oxides. XV. Al-for-Fe substitution in synthetic lepidocrocite: *Clays & Clay Minerals* **38,** (in press).

Taylor, R. M. and Schwertmann, U. (1978) The influence of aluminum on iron oxides. I. The influence of Al on Fe oxide formation from the Fe(II) system: *Clays & Clay Minerals* **26,** 373–383.

*(Received 17 November 1988; accepted 2 May 1989; Ms. 1853)*

*Note added in proof:* After acceptance of this manuscript, Mössbauer spectra of the samples with $0 < z < 0.11$ of series IV were taken at 160 K under a longitudinally applied magnetic field of 6 T. The measurements corroborate the results presented here insofar as they show the hyperfine fields of both tetrahedral and octahedral $Fe^{3+}$ to decrease with Al substitution, but they do not show an obvious preference of Al for either tetrahedral or octahedral sites.